Configuration Memory in Patchwork Dynamics for Low-dimensional Spin Glasses

Jie Yang, A. Alan Middleton
Department of Physics, Syracuse University, Syracuse, New York 13244, USA

A patchwork method is used to study the dynamics of loss and recovery of an initial configuration in spin glass models in dimensions $d = 1$ and $d = 2$. The patchwork heuristic is used to accelerate the dynamics to investigate how models might reproduce the remarkable memory effects seen in experiment. Starting from a ground state configuration computed for one choice of nearest neighbor spin couplings, the sample is aged up to a given scale under new random couplings, leading to the partial erasure of the original ground state. The couplings are then restored to the original choice and patchwork coarsening is again applied, in order to assess the recovery of the original state. Eventual recovery of the original ground state upon coarsening is seen in two-dimensional Ising spin glasses and one-dimensional Potts models, while one-dimensional Ising glasses neither lose nor gain overlap with the ground state during the recovery stage. The recovery for the two-dimensional Ising spin glasses suggests scaling relations that lead to a recovery length scale that grows as a power of the aging length scale.

arXiv:1703.09806v1 [cond-mat.dis-nn] 28 Mar 2017

Spin glass models are quintessential models for the study of disordered magnetic alloys, in the case where the interaction of magnetic moments has both frozen randomness and competition. The equilibrium and non-equilibrium behaviors of spin glass models are essentially different from those for homogeneous materials. For example, at zero temperature, the ground states do not exhibit conventional magnetic order but instead exhibit spatially randomly varying correlations of spins over long distances. The spin glass, whether it is a model or material, poses formidable challenges to the understanding of its complex non-equilibrium behaviors, including extremely slow dynamics and strongly history-dependent effects.[1] At low temperature, the full relaxation time for a spin glass material exceeds experimental time scales, though the slow approach to equilibrium can be studied in detail. A prototypical example of the resulting history-dependent effects is found in temperature cycling experiments.[2] If the otherwise uniform rate cooling of a spin glass material is paused, so that the sample is aged at a fixed temperature for a period of time before resuming further cooling, its magnetic susceptibility will vary slowly, "aging" with time. Upon further cooling and reheating, the magnetic susceptibility will return to its aged value as the temperature revisits the aging temperature, when the sample is reheated at a constant rate. That is, the sample can "recall" its temperature history. Numerous explanations for this memory effect have been presented.[3,4] Nonetheless, despite intensive study, many aspects of spin-glass dynamics remain poorly understood. As theoretical approaches, including droplet[5] and replica-symmetry-breaking[6] pictures, rely on distinct views of spin glasses and exact results are rare, numerical approaches have proven invaluable for verifying theories and motivating new ideas.[7]

Generic simulation approaches for spin glass models can also be excessively slow, due to the computational complexity of spin glass models. Finding the exact ground states of spin glasses in the general case is an NP-hard problem and so appears to require exponential time to solve. Finding ground states in three dimension can be impractical for more than a few thousand spins.[8–10] Direct Monte Carlo simulations, using single-spin-flip Glauber dynamics, have been used to explore the non-equilibrium spin configurations.[11] However, the evolution of a spin glass model under Glauber dynamics is extremely slow due to the high free-energy barriers between low free-energy configurations. Multiple applicable techniques for accelerating the process to equilibrium in spin glasses, such as parallel tempering[12] and simulated annealing,[13] have been developed but are also limited, though these techniques provide a wealth of information on the non-equilibrium behaviors of spin glasses. A fortunate exceptional case is the two-dimensional (2D) Ising spin glasses (ISG). Efficient algorithms that run in polynomial time do exist for exactly computing the equilibrium states of the 2DISG.[8,14] Here we exploit a fast local-equilibrium algorithm, "patchwork dynamics",[15] implemented here for zero temperature, to mimic the aging and memory effects in low-dimensional spin glass systems.

Patchwork dynamics is motivated by the expected dependence of free-energy barriers on length scale. For a domain with scale $\mathcal{L}$, the free-energy barrier $\mathcal{B}$ for the reversal of all spins is anticipated to scale as $\mathcal{L}^{\psi}$, where ψ is a barrier exponent.[5,16] At temperature T, a domain will then survive for a characteristic time $t \sim e^{\mathcal{B}/T}$, as thermal excitation is required to conquer the free-energy barrier. Given this exponential dependence on $\mathcal{L}$, a strong separation of time scales is provided by an examination of geometrically separated length scales. Patchwork dynamics uses this separation to replace a dependence on time scales by a dependence on length scales. This approach equilibrates the system at a given length scale directly using efficient equilibrium algorithms, which overcome large energy barriers quickly, rather than waiting for local single-site dynamics to slowly reach that length scale. By equilibrating collections of spins on a succession of increasing length scales, patchwork dynamics approximates the coarsening process. It takes advantage of efficient equilibrium algorithms to investigate the non-equilibrium behaviors of spin glasses. The evolution of spin glasses configurations is sped up, in a heuristic

fashion, by leaping over intermediate configurations with higher-free energies. We use this approach with the hope that it will provide us new insights into non-equilibrium behaviors of spin glasses.

In this paper, we investigate Ising spin glass systems on low-dimensional lattices: the square grid in two dimensions, the one-dimensional (1D) "chain" and the quasi-1D "ladder". We also examine the 1D m-state Potts spin glasses (PSG). For the ISG, the Hamiltonian is $\mathcal{H}_{\mathcal{I}} = -\sum_{\langle ij\rangle} J_{ij} s_i s_j$; for the PSG, the Hamiltonian has the form $\mathcal{H}_{\mathcal{P}} = -\sum_{\langle ij\rangle} J_{ij} \cos(\theta_j - \theta_i + \alpha_{ij})$. For all models, the couplings J_{ij} between nearest neighbor spins $\langle ij\rangle$ are mean-zero independent Gaussian random variables. The s_i and θ_i are spin variables on a d-dimensional lattice with $s_i = \pm 1$ and $\theta_i = \frac{2\pi n}{m}$, where $n = 1, \ldots, m$; the random noises α_{ij} between near neighbor spins for the PSG are random variables chosen from a uniform distribution on the interval $[0, 2\pi)$. Note that the ISG is equivalent to the standard PSG with $m = 2$ where the angle α_{ij} can be eliminated in the Hamiltonian. Highly efficient equilibrium algorithms exist for these spin glass systems in dimensions $d = 1$ and $d = 2$.[14,17]

Patchwork dynamics can be employed to attempt to replicate aging and memory effects. These dramatic history-dependent effects are typically observed in temperature cycling experiments. Similar effects are expected to be seen when the couplings are perturbed and then reverted rather than perturbing the temperature.[18,19] These behaviors are clearly related if temperature and disorder chaos[20] are related to the memory effects. At finite temperature, a small change in temperature leads to randomization of the coarse-grained couplings at the chaos scale. We mimic "temperature cycling" experiments by "disorder cycling", replacing the temperature chaos by the disorder chaos at $T = 0$.

Our simulation protocol is divided into two stages. The first stage is aging. We start with a ground state configuration for given couplings J_{ij} as our initial spin configuration. The ground states of the ISG are doubly degenerate, distinguished by a global spin flip,[21] while the m-state PSG possesses m-times degenerate ground states, related by spin rotation symmetry. The initial spin configuration is randomly chosen from the twofold (m-fold) ground state configurations (using the extended ground state with variable boundary conditions for the 2DISG[14]). We then change the couplings J_{ij} to an independently chosen set J'_{ij} , using disorder changes as a proxy for temperature changes. Patches are then applied using the new couplings J'_{ij} at a sequence of increasing scales ℓ. In each step of the sequence, we choose randomly located patches of length scale ℓ, and update the spins in that patch to the lowest energy configuration, given fixed spins at the boundary of the patch. For each ℓ, we apply $C(L/\ell)^d$ patches, with coverage $C = 20$. This ages towards a ground state for the new disorder J'_{ij} that is uncorrelated with the initial ground state for bond couplings J_{ij}. The second stage after this aging stage is recovery. We halt the aging process at a chosen patch size, the aging scale, and then the couplings are reverted to J_{ij}. Recovery advances by optimizing patches on successive length scales $r = 1, 2, 4, \ldots$, now using the original couplings. The maximum of r used is $L/2$, for a system of size L.

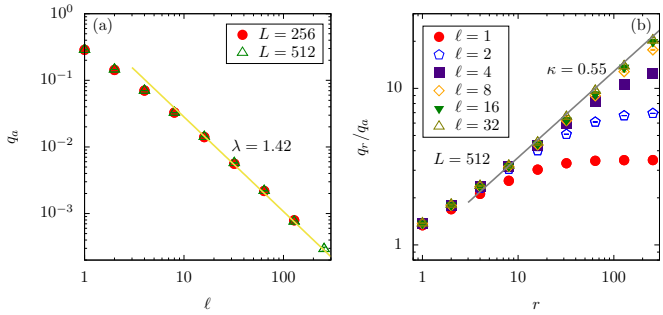

Figure 1: (Color online). Plot showing the sample-averaged spin overlap q of 2D Ising spin glass configurations with the initial ground state in the aging and recovery stages, using patchwork dynamics. (a) The spin configuration is initialized to a ground state configuration with couplings J_{ij} and is then aged with couplings J'_{ij} with patch sizes ℓ geometrically increasing. The ground states for bonds J_{ij} and J'_{ij} are uncorrelated. The spin overlap q_a with the ground state state for J_{ij} in the aging stage for sample size $L = 256$ and $L = 512$ decays consistently with a power law with a fitted exponent $-\lambda \simeq -1.42$. (b) For $L = 512$, we cease the aging stage at various scales $\ell = 1, 2, 4, 8, 16, 32$ and revert the couplings to J_{ij}. Under the patch dynamics with the original couplings, the spin configuration recovers to the original ground state for J_{ij}, not the oppositely oriented ground state, as indicated by the increasing overlap q_r with the ground state for J_{ij} during recovery. The spin overlap q_r initially grows in a fashion consistent with $q_r/q_a \sim r^{\kappa}$ with best estimated $\kappa \simeq 0.55$ at larger ℓ and r. This recovery crosses over to a plateau as $q_r \to 1$, seen in the data for smaller ℓ. The coverage parameter C of the patch dynamics, which is the number of times a single spin is included in some patch on average at each scale, was chosen to be $C = 20$.

The sample averaged spin overlap $q = N^{-1}\overline{\sum_i s_i^0 s_i}$ is a measure of the similarity of the initial ground state configuration s_i^0 with subsequent configurations s_i for the ISG, where N is the number of spins in the system. The 2DISG has $N = L \times L$ spins arranged on a square lattice with toroidal boundary conditions;[14] the chain IGS and the ladder IGS also have periodic boundary conditions and respectively have L and $k \times L$ spins where k is the number of layers of length L with open boundaries in the layer direction ($k = 2$ in the ladder ISG). In equilibrium, the overlap between two equilibrium configurations is used to extract thermodynamic behavior of spin glasses.[22] Here we use the overlap with the initial global ground state to quantify the aging and memory effects. For the 1DPSG, the spin overlap is chosen to be $q = N^{-1}\overline{\sum_i \cos(\theta_i^0 - \theta_i)}$. The θ_i^0 and θ_i are spin variables in the initial state and subsequent states, respectively; the number of spins is $N = L$ and periodic boundary conditions are imposed. The notation $q_a(\ell)$

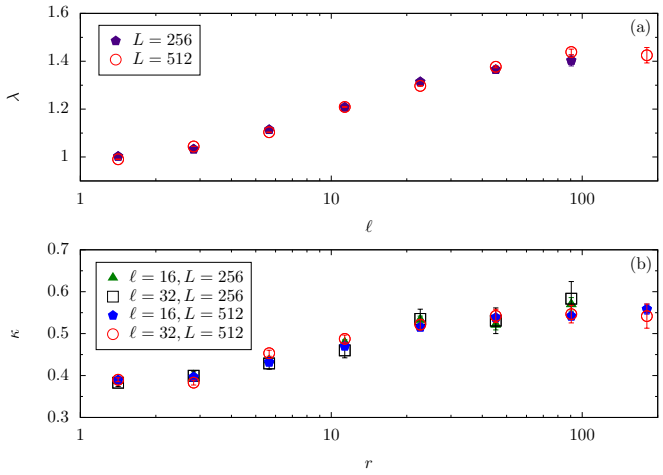

Figure 2: (Color online). Plots of local exponents λ and κ derived from neighboring data points plotted in Fig. 1 in the (a) aging and (b) recovery stages. The patch scales ℓ and r here are are the geometrical mean of two subsequent patch scales used to determine the local exponents. The local exponents $\lambda(\ell)$ and $\kappa(r)$ appear to plateau for ℓ and r greater 50. The small ℓ and r deviations are attributed to lattice effects. We extrapolate that under the limit of infinite sample sizes the exponents of 2D Ising spin glasses aging and recovery dynamics are $\lambda \simeq 1.42 \pm 0.08, \kappa \simeq 0.55 \pm 0.06$. Data shown are averaged over 10^5 samples.

and $q_r(r)$ will be used to denote overlaps computed in the aging stage at scale ℓ and the recovery stage at scale r, respectively.

Our patchwork heuristic aging and recovery procedures were applied to the 2DISG with sample sizes $L = 256, 512$. The behaviors of spin overlap q_a and q_r during aging and recovery shown in Fig. 1. In the aging stage, the decay of spin overlap q_a is well described by an asymptotic power law, $q_a \sim \ell^{-\lambda}$. This result is consistent with the conjecture introduced by Fisher and Huse,[5] where λ is an independent exponent of spin glass dynamics, and previous numerical results on 2D patch dynamics.[15]

In the recovery stage, we expect that the spin configuration will approach a ground state for J_{ij} as the patch size reaches L. However, it is undetermined whether the initial spin configuration $s_i = s_i^0$ or the reversed configuration $s_i = -s_i^0$ will be reached, given that the ground states are doubly degenerate. Since $q_r > 0$, our results indicate that samples approaching the initial spin configuration dominate those accessing the opposite ground state configuration, which statistically confirms that the 2DISG does have a memory of the initial spin configuration. We confirm that during the recovery stage the growth of spin overlap is well described by another asymptotic power law, $q_r/q_a \sim r^{\kappa}$.[15]

To attain an improved estimate of the scaling exponents λ and κ, we present the local exponents of spin overlap in Fig. 2. These are the slopes, $\frac{\Delta ln(q_a)}{\Delta ln(\ell)}$ and $\frac{\Delta ln(q_r)}{\Delta ln(r)}$, between two neighbor patch sizes. The patch sizes ℓ and r on the horizontal axes in Fig. 2 are the geometrical mean of the two subsequent patch sizes used to calculate the local exponent. The local exponents λ and κ are not constant at small ℓ and r and appear to crossover to a large distance limit for $\ell, r \geq 50$. We show power law fits in the corresponding regimes on Fig. 1. The estimated values are $\lambda = 1.42 \pm 0.08, \kappa = 0.55 \pm 0.06$, where systematic uncertainties are subjective and exceed the statistical error estimates at these length scales.

We observe in these latest simulations that as the maximum patch size ℓ decreases, the spin overlap in the recovery stage q_r diverges from the asymptotic power law seen for large ℓ. Instead, the spin overlap q_r crosses over to a plateau as patch sizes r increase at fixed small values of ℓ. The existence of this plateau is consistent with the spin configurations reaching the global ground state, which implies that the spin overlap $q_r \to 1$ at sufficiently large r. This suggests a scaling form for recovery that incorporates an initial power law increase followed by a plateau at $q_r = 1$. We emphasize that this scaling form assumes full recovery to the original spin direction with probability near 1, consistent with simulations for $r \gg \ell$. We also assume that the power law fits for aging and recovery are valid, so that the starting spin overlap $q_a(\ell)$ at the start of the recovery stage is $\ell^{-\lambda}$. This overlap then grows $q_r \sim r^{\kappa}\ell^{-\lambda}$ during recovery until this overlap q_r approaches unity. This leads to a crossover recovery scale r_c at patch size $r_c \sim \ell^{\frac{\lambda}{\kappa}}$ at which the spin overlap q_r approaches 1. The existence and scaling of this recovery scale is a central result of this current work. As $\lambda > \kappa$, the coarsening length scale for recovery r_c grows faster than the aging scale ℓ. The aging process erases the initial state sufficiently that the recovery scale, defined as the point where the overlap exceeds some fixed fraction of unity, say 1/2, must span a scale many times that of the aging scale, in the 2DISG.

Assuming a single recovery scale, scaling forms for both the spin overlap q_r and the domain wall bond density ρ in the recovery stage are fixed. Scaling collapses for these statistics are shown in Fig. 3, based on this description. The domain wall density is the fraction of bonds belonging to relative domain walls that separate ground states A, with spins s_i^0, and $\bar{A}$, with spins $-s_i^0$. The number of domain wall bonds in the 2DISG are taken to scale as r^{d_s}, with the domain walls for domains at recovery scale $r < r_c$ are taken to have the standard 2DISG domain wall fractal dimension $d_s \simeq 1.27$.[23,24] The domain wall bond density ρ thus scales as r^{d_s-2} until the recovery scale $r_c(\ell)$ is reached. To better describe our data following scaling collapses, we use the estimate $\lambda = 1.0$, the value of the effective exponent for small ℓ, given that our data show the plateau in Fig. 1 for small aging patch sizes, such as $\ell = 1, 2, 4$, along with the large r value $\kappa = 0.55$. We do not observe the scaling collapse for larger ℓ, because under that circumstance the patch size r_c that scales $r_c \sim \ell^{\frac{\lambda}{\kappa}}$ exceeds $L/2$ and thus is unreachable for our system sizes. The spin overlap q_r and domain wall bond

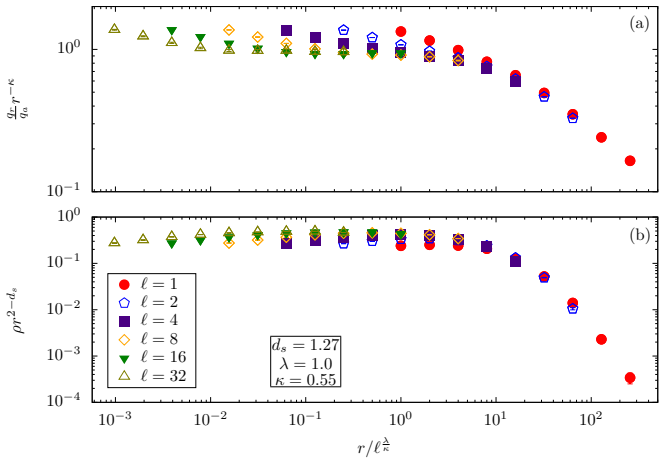

Figure 3: (Color online). Scaling collapses for (a) the spin overlap q_r and (b) domain wall bond density ρ in the recovery stage for sample size $L = 512$. For the patch size r smaller than the crossover length $r_c(\ell)$, the spin overlap scales as $\frac{q_r}{q_a} \sim r^{\kappa}$ with $\kappa \simeq 0.55$ and the domain wall bond density scales as $\rho \sim r^{d_s-2}$ with $d_s \simeq 1.27$. The statistics $\frac{q_r}{q_a} r^{-\kappa}$ and ρr^{2-d_s} are used to check the scaling $r_c \sim \ell^{\frac{\lambda}{\kappa}}$. The deviations at small scaling parameters are ascribed to lattice effects. We adopt here $\lambda \simeq 1.0$, which is the local exponent for small aging patch size ℓ, where we see a divergence from a simple power law at larger ℓ, where λ approaches $\lambda \approx 1.4$. The two statistics exhibit scaling collapses at an identical significant patch size r_c, which is consistent with our expectation.

density ρ in Fig. 3 both indicate an identical patch scale r_c where q_r approaches 1 and ρ vanishes rapidly from the scaling collapses, which corroborates our anticipated connection. Those points slightly deviating from a single curve for the scaling collapse at fixed values of r smaller than r_c are believed to stem from lattice effects. Overall, this scaling collapse with effective exponents for the domain wall density support a scaling picture for the recovery scale and for the relationship between domain wall density and recovery scale.

We have also carried out simulations to explore how the recovery depends on the sample preparation. For the results above (and those below for lower dimensional systems), we studied recovery after a specific coarsening process. This process decreases the spin overlap with the initial configuration by growing domains at the patch scale that are given by an independent set of spin couplings. For comparison, we have prepared samples by randomly selecting a subset of the initial spins and then flipping all of the spins in that subset. The size F of the subset chosen determines the overlap q with the initial configuration, via the relation $q = 1-2F/N$. There is no spatial correlation in which spins are flipped or remain unchanged. The overlap can be tuned arbitrarily without going through an aging process. We find that the recovery q_r from the chosen values for q are described by the same exponent κ, i.e., $q_r \sim q r^{\kappa}$. This suggests that the memory left after the aging process is not specific to coarse-graining towards another ground state. Isolated, uncorrelated remnant spins can be used to recover the initial configuration with the same quantitative growth of overlap.

To explore the effect of dimensionality on these non-equilibrium behaviors of spin glasses, we investigate memory effects on ISG systems with lower dimensionality, including the chain ISG and the ladder ISG. These two systems are both one-dimensional, with the ladder ISG system composed of two coupled chain ISG systems. Their ground states both consist of spins with statistically random orientations, as in the 2DISG. Nonetheless, there is a essential difference between their ground states. In the ground states of the chain ISG, all bonds but for at most one are satisfied. A bond is satisfied when neighbor spins on that bond are parallel if the bond coupling J_{ij} is positive, or they are in opposite orientations if J_{ij} is negative. Frustration results only from boundary conditions. The situation where a single bond with the minimum absolute value of J_{ij} is unsatisfied in the ground state of the chain ISG occurs with probability $\frac{1}{2}$ due to the randomness of the J_{ij}. With respect to the ladder ISG, conversely, frustrated plaquettes[8] commonly exist in its ground states. Bonds belonging to a frustrated plaquette cannot be all satisfied. Thus, the ground states of the ladder ISG include a finite density of unsatisfied bonds.

We apply the same patchwork dynamics protocols to the chain and the two-layer ($k = 2$) ladder ISG systems for sample sizes $L \leq 2^{17} = 262\,144$. The evolutions of spin overlaps for aging and recovery are displayed in Fig. 4. The spin overlap q_a for both the chain and the ladder ISG in the aging stage appear to follow power law decays, as seen in the 2DISG. The power laws for the two one-dimensional cases are similar to each other: The spin overlap q_a for both chain and ladder ISG are both well described by a single power law, $q_a \sim \ell^{-\lambda'}$ with a best fitted exponent $\lambda' = 1.00 \pm 0.03$. However, in the recovery stage the spin overlap q_r behave distinctly from each other at small recovery scales r. The recovery also differs at larger scales from that seen for the 2DISG (at all scales). To study the recovery of the spin overlap, we interrupt the aging at $\ell = 2, 4, 8$ and then revert the couplings to the original J_{ij}. The statistic q_r/q_a, the ratio of overlap in recovery to the overlap at maximal aging, of the chain ISG does not grow but stays fixed at 1, within our numerical error. This implies that the chain ISG does not show either any memory effects or any further aging under recovery coarsening. In contrast, the statistic q_r/q_a of the ladder ISG grows slightly and crosses over to a plateau $q_r/q_a \simeq 1.5$. Compared to the 2DISG, the memory effects for the ladder ISG are weak and do not trend to a power law at large recovery patch sizes. We have also studied the ISG with more layers, such as $k = 3$, where memory effects are apparently stronger than those of the two-layer ladder ISG, but we still find a plateau to a fixed ratio q_r/q_a during recovery. It is plausible to infer that the capability of memory grows and trends towards the full recovery seen in the 2DISG, as k increases.

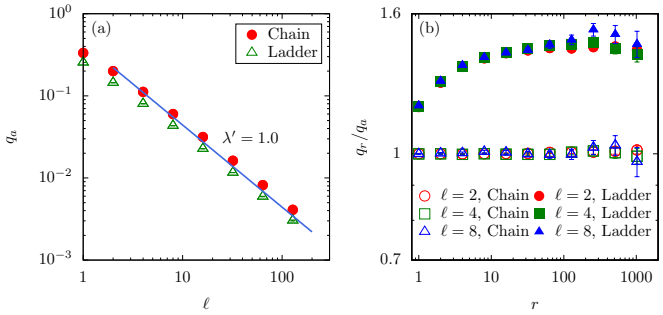

Figure 4: (Color online). Patchwork dynamics simulations on the chain and the ladder Ising spin glasses for sample size $L = 2^{17} = 262\,144$. (a) In the aging stage spin overlap q_a of the chain ISG and the ladder ISG behave similarly and are well interpreted by a power law, which is $q_a \sim \ell^{-\lambda'}$ with $\lambda' \simeq 1.0$. (b) In the recovery stage spin overlap q_r of the chain ISG and the ladder ISG have distinct behaviors. In both cases, the aging stage is terminated at various scales $\ell = 2, 4, 8$. For the chain ISG, the statistic q_r/q_a stays constant at $q_r/q_a \simeq 1$, which indicatess that the chain ISG does not possess memory recovery. However, the ladder ISG exhibits a weak initial memory effect. The statistic q_r/q_a slightly grows and crosses over to a plateau of 1.5, as is seen in the upper curves.

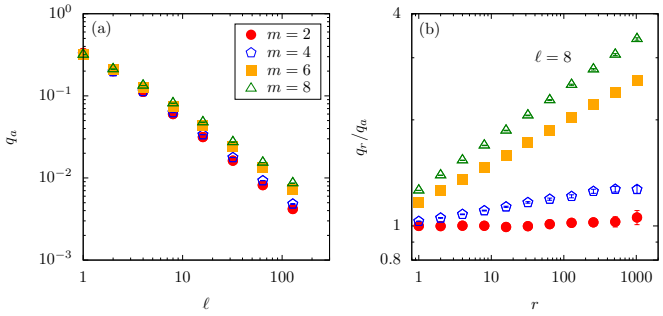

Figure 5: (Color online). Spin overlap q of 1D m-state Potts spin glasses in patchwork dynamics. The sample size is $L = 2^{17} = 262\,144$ and the number of spin states is $m = 2, 4, 6, 8$. (a) The spin overlap q_a decay as power laws $q_a \sim \ell^{-\lambda_{\mathcal{P}}}$ in the aging stage. The exponent $\lambda_{\mathcal{P}}$ slightly decreases, as m increases. (b) The spin overlap q_r in the recovery stage show significantly difference for various m. In the data displayed, we cease the aging at $\ell = 8$. The absence of memory effect is indicated for $m = 2$ as in the case of the chain Ising spin glasses. The spin overlap q_r for $m = 4, 6, 8$ can be well described by power laws $q_r/q_a \sim r^{\kappa_{\mathcal{P}}}$, with small κ. The 1D Potts spin glasses show the recovery of memory for $m = 4, 6, 8$. The exponent $\kappa_{\mathcal{P}}$ grows as the spin degrees of freedom m increase (see text), which indicates weak reinforcement of memory with the increase of m.

We find it interesting that the chain ISG shows no memory in our simulations. To explain this absence of memory, we calculate analytically the expected change of spin overlap when patches of arbitrary size r are applied during the recovery stage. This expected change can be computed for an arbitrary spin configuration. Given a spin configuration in a given sample with fixed J_{ij}, we define Δ_i as the change of spin overlap q_r caused by optimizing the spins in a patch with size r starting at position $i+1$, that is, with boundary spins s_i and s_{i+r+1} fixed. The average $\langle \Delta_i \rangle$ is then defined as the expectation value of the change in the spin overlap, where the angle brackets indicate an average over the position i. We will use the symbol $+$ for a spin of the same sign as in the ground state configuration; the symbol $-$ means a spin has the opposite orientation. The overlap can be found from the sum of the number n_+ of $+$ spins, with $q = L^{-1}(2n_+ - 1)$. There are L different patches with size r and they can be classified into four categories, one for each patch boundary condition. Boundary conditions for these categories are indicated by $++$, $--$, $-+$ and $+-$, with the two symbols referring to the relative orientation of two boundary spins for the linear patch with respect to the ground state configuration. The number of four different categories of patches in a given sample and given r are respectively n_{++}, n_{--}, n_{-+} and n_{+-}. When a patch is applied, the value of Δ_i depends on the category and the spins inside the patch. All spins in patches with boundary conditions $++$ will be set to $+$; spins in patches with boundary conditions $--$ will have a post-patch orientation of $-$; for patches with boundary conditions $+-$ or $-+$, a domain wall will result at $b(i,r)$ where $b(i,r)$ is the relative location for the local minimum of J_{ij} within the given patch. The sign of the spin with respect to the ground state changes between the spin with index $i + b(i,r)$ and the spin with index $i + b(i,r) + 1$. We use the notation $\sum_{i,+-}$ to indicate a sum over all i restricted to patches of type $+-$, for example. When a patch forces a spin s_k to be $+$, the change in overlap is $(1 - s_k)/L$. and when a patch forces a spin s_k to be $-$, the change in overlap is $(-1 - s_k)/L$. Thus, given a uniform probability over location for the placement of patches, $\langle \Delta_i \rangle$ can be written as

$$
\begin{aligned}
\langle \Delta \rangle &= \frac{1}{L} \sum \Delta_i \\
&= \frac{1}{L} \Bigg(\sum_{i,++} \sum_{k=i+1}^{i+r} (1 - s_k) + \sum_{i,--} \sum_{k=i+1}^{i+r} (-1 - s_k) \\
&\quad + \sum_{i,-+} \left[\sum_{k=i+1}^{i+b(i,r)} (-1 - s_k) + \sum_{k=i+b(1,r)+1}^{i+r} (1 - s_k) \right] \\
&\quad + \sum_{i,+-} \left[\sum_{k=i+1}^{i+b(i,r)} (1 - s_k) + \sum_{k=i+b(1,r)+1}^{i+r} (-1 - s_k) \right] \Bigg) \\
&= \frac{r}{L} \left(- \sum s_k + n_{++} - n_{--} + n_{-+} - n_{+-} \right) \\
&\quad + \frac{2}{L} \left(\sum_{i,+-} b(i,r) - \sum_{i,-+} b(i,r) \right) . \qquad (1)
\end{aligned}
$$

Letting N_+ and N_- be the number of up and down spins, respectively, the number of patch categories is con-

strained by the equations

$$2n_{++} + n_{+-} + n_{-+} = 2N_+ \quad (2)$$
$$2n_{--} + n_{+-} + n_{-+} = 2N_- \quad (3)$$
$$N_+ - N_- = \sum s_k \,, \quad (4)$$

from counting the contributions of each type of patch category to the total number of up or down spins (Eq. (2) and Eq. (3)) and from the definitions of N_+ and N_- (Eq. (4)). It follows from Eqs. (2-4) that

$$-\sum s_k + n_{++} - n_{--} = 0 \,. \quad (5)$$

It is also true, for a given sample, due to the periodic boundary condition, that

$$n_{-+} = n_{+-} \,. \quad (6)$$

To show this, the set of sites $\{1, \ldots, L\}$ can be decomposed into distinct orbits $O_1, O_2, \ldots$, where each orbit O_m is a sequence of sites $O_m = \{i_m + k(r+1) \mod L | k = 0, 1, \ldots\}$. These orbits are sets of the left ends of patches where the patches share boundary points. As L is finite, each O_i is finite. In each orbit O_i, there must be an equal number of $+-$ and $-+$ patches. Since n_{+-} and n_{-+} is the sum of these counts over the set of orbits, we have $n_{-+} = n_{+-}$.

Using Eq. (5) and Eq. (6), we can write the expected change in overlap for a patch of size r in a given sample, $\langle \Delta(J_{ij}) \rangle$, as

$$\langle \Delta(J_{ij}) \rangle = \frac{2}{L} \left(\sum_{i,+-} b(i,r) - \sum_{i,-+} b(i,r) \right) . \quad (7)$$

The distance to the domain wall for mixed boundaries $b(i,r)$ can take any integer value in the range $[0, L-1]$. In an individual sample, it is likely that $\sum_{i,+-} b(i,r) \neq \sum_{i,-+} b(i,r)$. However, if we average over a large number of samples, the mean change of the spin overlap $\langle \Delta(J_{ij}) \rangle = 0$, due to the statistical left-right symmetry that does not on average distinguish $-+$ from $+-$ boundary points. We conclude that during patch dynamics for the 1DISG, the overlap with the ground state for the J_{ij} used does not change. This analytic result is consistent with our simulation results for the recovery phase.

We have also explored how the symmetry of the spin degrees of freedom (DOF) affects the recovery of memory in spin glasses. We employ our patch aging/recovery protocols on the 1DPSG with varying number of single spin states, $m = 2, 4, 6, 8$. In the ground states of the 1DPSG with $L > 2m$, the bonds are mostly all satisfied, as the periodic boundary conditions can lead up to m unsatisfied bonds. These ground states are m-fold degenerate. The spin overlap in coupling cycling simluations are exhibited in Fig. 5. In the aging stage, the spin overlap q_a is well fitted by power laws, $q_a \sim \ell^{-\lambda_{\mathcal{P}}}$. A local exponent analysis shows that, as the number of spin states m increases, the local power law exponent $\lambda_{\mathcal{P}}$ marginally decreases with increasing m, though perhaps within systematic uncertainties. For example, quantitatively, the fitted exponent $\lambda_{\mathcal{P}} \simeq 0.97, 0.94$ for $m = 2, 4$ respectively. We then study the behavior of spin overlap q_r in the recovery stage after halting the aging at $\ell = 8$. The 1DPSG with $m = 2$ exhibits no memory effects, as in the case of the chain ISG, though the Hamiltonian is slightly different from the ISG case. For $m > 2$, the 1DPSG exhibits memory effects and the statistic q_r/q_a is plausibly described by a small power law growth for recovery, $q_r/q_a \sim r^{\kappa_{\mathcal{P}}}$. A logarithmic growth of the recovery ratio with r is possible, though the fit is less good. The strength of memory exhibits some enhancement as m increases over the range we studied , as is seen in Fig. 5; the estimated scaling exponent $\kappa_{\mathcal{P}} \simeq 0.14$ with $m = 8$ is greater than $\kappa_{\mathcal{P}} \simeq 0.12$ with $m = 6$.

In conclusion, patchwork dynamics provides an efficient heuristic technique to investigate the nonequilibrium behaviors of large spin glass systems, which are more difficult to study at large scales using conventional Monte Carlo methods. We use patchwork dynamics to mimic the cooling and reheating processes on spin glass materials. The spin overlap and domain wall density show memory effects, as magnetic susceptibility does in experiments.[2] We expand upon the scaling description of the aging and recovery stages, consistent with numerical evidence. In particular, we identify a recover scale r which grows as a power law of the aging scale ℓ, $r \sim \ell^{\lambda/\kappa}$, where λ is the decay exponent for the spin overlap during aging and κ is the overlap recovery exponent. As the exponent ratio $\lambda/\kappa \approx 2.58$, the recovery scale grows much more quickly than the aging scale. Thus recovery of the original spin direction requires coarsening to a scale that grows faster than the aging scale that causes erasure. We note that the recovery exponent κ is independent of whether the erasure is caused by coarsening through aging or through random flipping of the spins. We have also studied how the dimensionality and the spin symmetry affect the strength of memory in various spin glass models. It is notable that the chain ISG shows the exact absence of memory effects. The ladder ISG whose dimensionality is between 1D and 2D exhibits weaker memory effects than the 2DISG. Simulations results from the one-dimensional Potts spin glass indicate that memory effects become stronger as the number of spin states increases.

---

[1] *Spin Glasses and Random Fields*, edited by A. P. Young (World Scientific, Singapore, 1998).

[2] V. Dupuis, F. Bert, J.-P. Bouchaud, J. Hammann, F. Ladieu, D. Parker and E. Vincent, Pramana J. Phys. **64**, 1109 (2005).

[3] E. Vincent, *Ageing and the Glass Transition*, edited by M. Henkel, M. Pleimling, and R. Sanctuary (Springer, Berlin, 2007).

[4] P. E. Jönsson, R. Mathieu, P. Nordblad, H. Yoshino, H. A. Katori, A. Ito, Phys. Rev. B **70**, 174402 (2004).

[5] D. S. Fisher and D. A. Huse, Phys. Rev. B **38**, 386 (1988).

[6] G. Parisi, Phy. Rev. Lett. **50**, 1946 (1983).

[7] *New Optimization Algorithms in Physics*, edited by A. K. Hartmann and H. Rieger (Wiley-VCH, Weinheim, 2004).

[8] F. Barahona, J. Phys. A **15**, 3241 (1982).

[9] C. H. Papadimitriou, *Computational Complexity* (Addison-Wesley, Reading, MA, 1994).

[10] F. Liers, M. Palassini, A. K. Hartmann, and M. Junger, Phys. Rev. B **68**, 094406 (2003).

[11] E. Marinari, G. Parisi, and J. J. Ruiz-Lorenzo, Phys. Rev. B **58**, 14852 (1998).

[12] R. H. Swendsen and J.-S. Wang, Phys. Rev. Lett. **57**, 2607 (1986).

[13] S. Kirkpatrick, C. D. Gelatt, and M. P. Vecchi, Science **220**, 671 (1983).

[14] C. K. Thomas and A. A. Middleton, Phys. Rev. B **76**, 220406 (2007).

[15] C. K. Thomas, O. L. White, and A. A. Middleton, Phys. Rev. B **77**, 092415 (2008).

[16] R. Paul, G. Schehr, and H. Rieger, Phys. Rev. E **75**, 030104(R) (2007).

[17] M. Suzuki, Phys. Rev. B **31**, 2957 (1985).

[18] H. Yoshino, A. Lemaitre. and J.-P. Bouchaud, Eur. Phys. J. B **20**, 367 (2001).

[19] H. G. Katzgraber and F. Krzakala, Phys. Rev. Lett. **98**, 017201 (2007).

[20] A. J. Bray and M. A. Moore, Phys. Rev. Lett. **58**, 57 (1987).

[21] D. S. Fisher and D. A. Huse, J. Phys. A **20**, L997 (1987).

[22] A. A. Middleton, Phys. Rev. B **87**, 220201(R) (2013).

[23] A. A. Middleton, Phys. Rev. B **63**, 060202(R) (2001).

[24] A. K. Hartmann and A. P. Young, Phys. Rev. B **66**, 094419 (2002).